Hydrological conditions control *in situ* DOM retention and release along a Mediterranean river

A. Butturini [a, *], A. Guarch [a], A.M. Romaní [b], A. Freixa [b], S. Amalfitano [c], S. Fazi [c], E. Ejarque [d, e]

[a] Departament d'Ecologia, Universitat de Barcelona, Barcelona, Spain
[b] Institute of Aquatic Ecology, Department of Environmental Sciences, University of Girona, Girona, Spain
[c] Water Research Institute, National Research Council of Italy (IRSA-CNR), Monterotondo, Roma, Italy
[d] WasserCluster Lunz, Biologische Station GmbH, Lunz am See, Austria
[e] Department of Limnology and Bio-Oceanography, University of Vienna, Austria

ARTICLE INFO

ABSTRACT

Uncertainties exist regarding the magnitude of *in situ* dissolved organic matter (DOM) processing in lotic systems. In addition, little is known about the effects of extreme hydrological events on in-stream DOM retention or release during downriver transport.

This study quantified the net in-stream retention/release efficiencies (η) of dissolved organic carbon (DOC) and its humic and protein-like fluorescent fractions along a Mediterranean river during drought, baseflow and flood conditions. High performance size exclusion chromatography was used to describe the apparent size distributions of the humic and protein-like DOM moieties. A snapshot mass balance allowed estimating the η values of DOC and humic and protein-like fractions. Significant DOM net retention ($\eta < 0$) was detected during the drought condition and the protein-like fraction was more retained than the humic-like fraction and bulk DOC. In addition, small substances were more efficiently retained than larger substances. DOC retention decreased under baseflow conditions, but it remained significant. The humic and protein-like net efficiencies exhibited high variability, but the net retention were not significant. From a longitudinal perspective, the entire fluvial corridor contributed net retention of DOC and humic and protein-like moieties net retention during drought condition. In contrast, net retention/release efficiencies exhibited spatial variability during baseflow condition. The flood preferentially mobilized large size DOM molecules and the fluvial corridor behaved as a homogeneous passive DOM ($\eta = 0$) conduit.

This research highlights the relevance of hydrological extreme events on the magnitude of DOM retention/release mass balance and emphasizes the need to perform measurements during these conditions to quantify the impact of fluvial corridors on DOM fate and transport.

1. Introduction

Dissolved organic matter (DOM) comprises a complex mixture of organic substances that represent basic resources for carbon and energy in fluvial ecosystems. Most of the DOM that flows in rivers originates in the terrestrial environments (Gordon and Goni, 2003). However, in-stream biotic and abiotic processes modulate its availability, transport, release and retention, and significantly affect the carbon cycle at the fluvial (del Giorgio and Pace, 2008) and global scales (Battin et al., 2009). DOM uptake by heterotrophic microbes is essential for introducing dissolved carbon into the detritus-based food webs (Findlay, 2010). Aquatic microbes also actively release amino acids, proteins (del Giorgio and Pace, 2008) and low molecular weight humic-like substances (Fasching et al., 2014). Organic exudates from aquatic plants, phytoplankton and animal excrements provides additional autochthonous DOM sources (Elliott et al., 2006; Fisher et al., 2004). UV radiation can alter DOM composition (Gonsior et al., 2009), by degrading humic substances (Meng et al., 2013) and promoting the formation of low-molecular weight substances (Bertilsson and Tranvik, 2000) and reactive excited state matter (Bodhipaksha et al., 2015) or oxidizing DOM to CO_2 (Miller and Zepp, 1995).

Molecular size is considered a relevant parameter for DOM reactivity. Heterotrophic microbes preferentially take up small

---

* Corresponding author.
E-mail address: abutturini@ub.edu (A. Butturini).

molecules because they cannot directly assimilate molecules larger than 0.5—1 kDa (Marschner and Kalbitz, 2003; Seitzinger et al., 2005). Extracellular enzymes are released to specifically degrade larger molecules (Romaní et al., 2012). However, DOM chemical structure or physical protection may further limit its biodegradation (Nebbioso and Piccolo, 2013) limiting, for instance the availability of low molecular weight compounds for bacterial uptake (Waiser and Robarts, 2000). Therefore, a consistent relationship cannot be ascertained between DOM molecular size and its bioavailability/reactivity (Fischer et al., 2002; Attermeyer et al., 2014). However, the "size-reactivity continuum" conceptual model (Amon and Benner, 1996, hereafter SRC model) suggests that large molecules are more susceptible to transformation.

DOM processing is difficult to predict in the river continuum context. An increase of recalcitrant molecules and a decrease in DOM processing is expected downriver (Vannote et al., 1980; Fellman et al., 2014). Thus, the SRC model (Amon and Benner, 1996) suggests that larger and reactive molecules are more prevalent at the headwaters, while smaller and recalcitrant molecules are significant downriver. However, this scenario may be altered by the succession of natural and anthropogenic inputs from tributaries (Fisher et al., 2004) which can interrupt the biogeochemical fluvial continuum adding DOM with distinct composition and molecular size. These inputs are mainly controlled by the frequency, timing and magnitude of hydrological events. For example, low DOM processing is expected during floods due to the short water residence times. In contrast, long water residence times should stimulate in-stream DOM processing and autochthonous production during droughts. Additionally, DOM inputs from tributaries and anthropogenic sources are expected to determine the input of a highly heterogeneous mixture of DOM of large, medium and small organic substances during drought and baseflow periods. Therefore, a detailed longitudinal hydrological biogeochemical monitoring under these hydrological conditions can provide evidence, under *in situ* conditions, about the relevance of DOM molecular size on its reactivity.

Despite an increasing interest in the quantitative and qualitative DOM variations along a fluvial continuum (Fellman et al., 2014; Creed et al., 2015; Wollheim et al., 2015), two main gaps in our knowledge exist:

1) A large uncertainty exists regarding the magnitude of *in situ* DOM retention/release in lotic systems. The majority of the current knowledge is based on *ex situ* laboratory bioassays, meanwhile *in situ* DOM mass balances in large fluvial segments have been executed only sporadically (Kaushal et al., 2014; Sirivichi et al., 2011) and no studies have extended these assessments to humic and protein-like moieties across the molecular size spectrum.
2) Studies have generally been performed under baseflow conditions (Temnerud et al., 2009; Wollheim et al., 2015), whereas droughts (Vazquez et al., 2011 and 2015) and more especially, floods have been rarely investigated. Extreme hydrological events significantly impact DOM inputs to rivers (Raymond and Saiers, 2010; Fasching et al., 2015). Therefore, the biogeochemical functioning of rivers can only be fully understood by integrating information over a broad range of hydrologic conditions.

Based on these two shortcomings, the goal of this study was to estimate the net in-stream DOM retention/release efficiencies during drought, baseflow and flood conditions along a large fluvial segment of a Mediterranean river. Snapshot sampling campaigns (Grayson et al., 1997) were performed to obtain DOM reach-scale mass balances. High performance size exclusion chromatography (HPLC-SEC) was used to describe changes in the apparent size distributions of humic and protein-like DOM substances. We hypothesized that

protein-like fractions should be retained more than the humic-like fractions (Cory and Kaplan, 2012). In addition, according to the SRC model (Amon and Benner, 1996), within a specific type of substances (i.e. protein- or humic-like), large molecules should be more susceptible to be transformed downriver than the smaller ones.

2. Materials and methods

2.1. Study site

This study was conducted in the Tordera, a human-impacted Mediterranean river that drains into the Mediterranean Sea. This river is located 70 km to the northeast of Barcelona (Catalonia, Spain) and it drains a catchment area of 870 km^2, which extends to the south-eastern faces of the Montseny and Guilleries massifs (up to 1712 m a.s.l.) and the northern slopes of the smaller Montnegre massif (773 m a.s.l) (Fig. 1). The main river stem is 60 km long with a shallow water column (typically less than 0.5 m). Riparian vegetation shades the river bed during the first 25 km, where the active river channel is 2—8 m wide. The river floodplain width increases up to 100—130 m near the river mouth where the river becomes braided. Accordingly, riparian shading is unimportant along the majority of the main stem. The river sediment is dominated by a highly permeable gravel and sand (Vannak, 2015). The river receives the most important lateral inputs in the central portion of the main stem, which is located between kilometre 19 (170 m a.s.l.) and kilometre 45 (36 m a.s.l.). These inputs include intermittent pristine tributary streams, anthropogenically permanent tributary streams and effluents from industrial and waste water treatment plants (WWTPs). The catchment narrows and the lateral surface inputs are minimal from kilometre 45 to the river mouth. This final fluvial segment is typically dry during the summer. According to the continuous discharge records from the Catalan Water Authority (ACA), drought conditions were typically observed for approximately 25% of the total days over the last ten years and contributed to 3% of annual water export. Conversely, baseflow (65% of the time) and flood (10% of the time) conditions contributed 42 and 55% of the annual water export, respectively (Fig. 1b).

2.2. Sampling strategy and river discharge measurements

The Tordera was sampled three times, during drought, baseflow and flood conditions. The three sampling campaigns spanned four orders of magnitude of river flow. Table 1 provides water velocities and residence time data for the three hydrological conditions. Drought sampling was performed during a summer drought episode when the water flow was low and absent at the most downriver sites. The flood event represented the largest flood recorded over the last 10 years (according to data provided by ACA). Therefore, the three sampling campaigns spanned the spectra of hydrological conditions in the system (Fig. 1b).

Water samples were collected from 19 to 21 sites distributed along the entire main reach extending from headwaters (530 m a.s.l.) to the river mouth (0 m a.s.l.). The mass-balance was performed for the central and lowest portions of the main reach (Fig. 1). No large artificial barriers that may alter the water flow exist in this fluvial segment. The river typically recharges the adjacent alluvial aquifer at most sites (Mas-Pla and Menció, 2009) and water inputs from groundwater should be negligible.

The mass balance started at kilometre 19. During the drought sampling, the river continuum became fragmented into disconnected pools from kilometre 42 and totally dry from kilometre 50. The installation of a large gas pipeline in the river bed at kilometre 36 rendered downriver mass balance calculations unfeasible. Therefore, the mass balance ended at kilometre 35. The mass
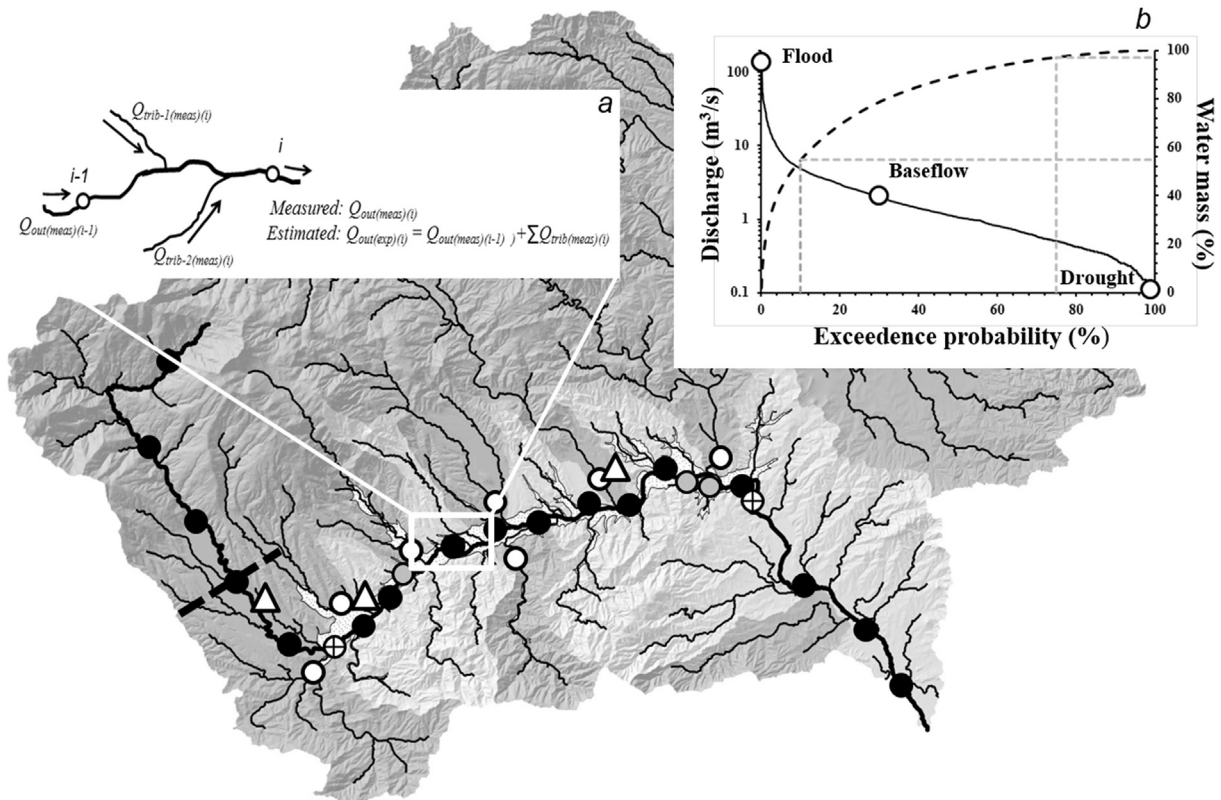
Fig. 1. Catchment of the La Tordera river and location of the sampling sites along the main stem and tributaries (both natural and anthropogenic). Black dots are the main river sampling sites: white dots are the sampled tributaries; gray dots are industrial outlets; White triangles are waste water treatment outlets; Crossed white dots are the discharge gauging stations (Agencia Catalana Aigua). Dashed black line indicates the position of the upriver boundary of the snapshot mass balance. Inset *a* shows a schematic representation of calculation of the expected discharge at the outlet of reach "*i*" ($Q_{out(exp)(i)}$). See the text for additional details. Inset *b* shows the discharge probability distributions (DPDs) based on ten years hydrological data from the downriver gauging station (kilometre 45, data provided by the Agencia Catalana Aigua). Solid black line shows the instantaneous discharge distribution. Dashed line shows the accumulated water mass distribution. White dots indicate the position of the three sampled episodes. Dashed gray lines split the DPDs into drought, baseflow and flood periods.

Table 1
Hydrological conditions during the three surveys.

Date	Flow condition	Discharge[a] (m³/s)	Water velocity (m/s)	River segment length[b] (km)	Water residence time [c] (h)	River bed area[c] (km²)
07/11/2012	Drought	0.011	0.12 ± 0.07	16 (from km 19 to km 35)	100	0.12
4/26/2012	Baseflow	0.9	0.42 ± 0.2	39 (from km 19 to km 58)	24	0.25
03/06/2013	Flood	73	0.83 ± 0.23	26 (from km 19 to km 45)	11	1.6

[a] Discharge values from the sampling site at kilometre 37.
[b] Length of the river segment selected for the mass balance.
[c] Values related to the river segment length selected for mass balance. See text for details.

balance extended to the river mouth (kilometre 58) during baseflow, but ended at kilometre 45 during flood because the large flood made it impossible to accurately estimate the discharge in the farthest downriver reaches (Table 1).

All known lateral surface inputs were sampled. Inputs included all the major tributaries and anthropogenic sources (Fig. 1). The sampled anthropogenic effluents included three WWTPs (at kilometres 20.5, 25 and 37) and three industrial outlets (at kilometres 26, 40 and 41). All inputs were sampled before discharging to the main stem. The sampled tributaries combined drain 85% of the total catchment area. The remaining unsampled tributaries include small intermittent streams located in the southern portion of the catchment. The water and solute mass contributions of the unsampled tributaries were interpolated from the specific discharges and mass fluxes of adjacent sampled sub-catchments according to Emerson et al. (2005).

All sampling campaigns were executed in less than four hours. The discharge was calculated at each sampling site using the velocity-area method (Di Baldassarre and Montanari, 2009). A flowmeter (Global Water FP111 Flow, sensor range 0.1—6.1 m/s) was used to measure the mean water velocity. The river channel cross section was divided into 0.2—0.5 m width (depending of the river width) subsections. The mean water velocity was estimated at 50% of the total depth. The standard error of the discharge measurement was 7% at each sampling site, which is similar to the values reported by Di Baldassarre and Montanari (2009). The discharge estimation errors were estimated during preliminary hydrological campaigns executed under baseflow and drought conditions.

Conditions during the flood made it impossible to take in-river measurements with a flow meter. In this case, discharges were estimated using the Manning's equation (Chanson, 2004). Photographs of the river channel were taken at each sampling site during the flood and these were later used to measure the cross-sectional flow area and the wetted perimeter at each sampling site. The Manning's coefficient was set to 0.05, corresponding to natural

channels with sluggish reaches and stones (Chow, 1959). The river channel gradient was estimated by applying the communicating vessel principle to a large pipe (40 m) filled with water. Additionally, main stem discharge was continuously recorded by ACA at kilometres 24 and 46. These discharge values served as a reference to validate our discharge calculations.

2.3. Chemical analyses and DOM fractionation

Water samples were manually collected and immediately filtered using pre-combusted GF/F (Whatman) fiberglass filters (0.7 μm pore size) for the total dissolved organic carbon (DOC) analysis, and 0.22 μm pore nylon filters for the molecular weight distribution analysis. An aliquot of 30 ml was acidified 3% v/v using 2 M HCl and refrigerated before DOC analysis. DOC was analyzed using a Shimadzu TOC Analyser VCSH. Water electrical conductivity was measured *in situ* using a WTW Cond 3310 Set 1.

High-pressure liquid size exclusion chromatography (HPLC-SEC) was used to describe the DOM humic-like and protein-like moieties based on the molecular weight (MW) (Allpike et al., 2005). The HPLC utilized a Jasco PU-2089 HPLC system equipped with a FP-2020 fluorescence detector. DOM molecular size separation was performed with two Polysep-GFC Phenomenex columns (P3000 and P5000, 600 × 7.8 mm) in series. The eluent consisted of 10 mM ammonium acetate adjusted to pH 7. The mobile phase was filtered using 0.22 μm pore nylon membranes. The injection volume was 100 μL. The samples ionic strength was adjusted to 10 mM using a concentrated solution of ammonium acetate (Her et al., 2003).

Three standards (polystyrenesulfonic acid sodium salts, Sigma-Aldrich) with known molecular weights (0.21, 4.3 and 6.8 kDa) were used to calibrate the columns and to have an approximate estimate of the molecular weight of our samples. However, standards do not travel through the columns in the same manner as DOM molecules. Therefore the molecular weight range described in this paper is based on the apparent DOM size and should be considered for comparative purposes only (Romera-Castillo et al., 2014).

The DOM size distribution was analyzed in terms of fluorescence. In accordance with a previous study performed in the same river (Ejarque-Gonzalez and Butturini, 2014), we focused on a humic-like peak ($\lambda_{ex}/_{em}$ = 360/460) and protein-like peak ($\lambda_{ex}/\lambda_{em}$ = 285/340). The protein-like peak corresponds to the tryptophan peak (Coble, 1996). Each sample was analyzed twice.

2.4. Mass balance

The river segment selected for the water and DOM mass balances was split into consecutive reaches according to the location of the main confluences with lateral inputs. The length of the reaches ranged from 0.66 to 4.25 km. A snapshot mass balance (Grayson et al., 1997) was calculated at each reach to estimate the net in-stream DOM retention/release efficiencies.

2.4.1. Water mass balance computation

The discharge measured at the output of each reach i ($Q_{out(meas)(i)}$) was compared with two expected discharge values to quantify the contribution of inputs from tributaries and groundwater.

The first expected discharge parameter was the "reach scale expected discharge" ($Q_{out(exp)(i)}$). $Q_{out(exp)(i)}$ was the sum of the measured discharge from the output of the previous reach i-1 ($Q_{out(meas)(i-1)}$) and the discharge from all identified inputs that delivered water in that reach ($\sum Q_{trib(meas)(i)}$; Fig. 1a):

$$Q_{out(exp)(i)} = Q_{out(means)(i-1)} + \Sigma Q_{trib(means)(i)} \quad \left[\text{volume time}^{-1}\right]$$
(1)

The difference $\Delta Q_{(i)} = Q_{out(exp)(i)} - Q_{out(meas)(i)}$ indicated the contribution of water flow from groundwater or an unsampled water input. $\Delta Q_{(i)} > 0$ suggested that the river recharged the aquifer. This relationship did not alter the solute mass balance (see below) because it did not represent a groundwater mass input. The Tordera alluvial aquifer is exploited by human activities and $\Delta Q_{(i)} > 0$ is the typical situation (Mas-Pla and Menció, 2009). In contrast, $\Delta Q_{(i)} < 0$ indicated that the aquifer recharged the river and groundwater input must be included in equation (1). Representative solute concentrations were difficult to obtain in groundwater during river sampling. Therefore, we assumed that if $\Delta Q_{(i)} < 0$ and $\Delta Q_{(i)}/Q_{out(meas)(i)}$ was larger than 7% (i.e. the standard error of discharge measurements) at reach i, then the groundwater input could not be ignored and the mass balance of the reach was removed from the calculations (see results 3.1 for details).

The second expected discharge parameter was the "accumulated expected discharge" ($\sum Q_{out(exp)(i)}$). This parameter was obtained by taking into account the discharge measured at all lateral inputs. $\sum Q_{out(exp)(i)}$ was assumed to be the sum of all lateral inputs located upstream of sampling site i. The $\sum Q_{out(exp)(i)}$ computation does not use discharge values from the river main stem but assumes that the main stem is a conduit that channelizes water flow from tributaries without groundwater exchange. The plot of $\sum Q_{out(exp)(i)}$ versus $Q_{out(meas)(i)}$ illustrates the contribution of the lateral inputs to the river discharge. A good fit along the line 1:1 suggests that river discharge was function of lateral water inputs and that groundwater did not significantly recharge the main stem. In contrast, if data were located below the 1:1 line, a diffuse and extended input from an unknown water source may exist (e.g. groundwater). Data located above the 1:1 line would indicate that the river recharged the aquifer.

2.4.2. Net in-stream DOM retention/release efficiencies

The DOM mass balance was performed via the following calculations. In each reach i the inputs of solute y were the sum of the fluxes of y from the output of the previous reach i-1 ($m_{inp(meas)(y, i-1)}$) and from all tributaries ($\sum m_{trib(meas)(y, i)}$) that add inputs to the reach:

$$m_{inp(y,i)} = m_{out(meas)(y,i-1)} + \Sigma m_{trib(meas)(y,i)} \quad \left[\text{mass time}^{-1}\right]$$
(2)

The mass fluxes ($m_{out(meas)(y,i-1)}$ and $m_{trib(meas)(y,i)}$) are the product of the water discharges $Q_{out(meas)(i-1)}$ and $Q_{trib(meas)(i)}$ (eq. (1)) and the measured solute concentration y at the previous (i-1) sampling site ($C_{out(meas)(y,i-1)}$) and tributaries ($C_{trib(meas)(y,i)}$).

The expected concentration of the solute y ($C_{exp(y,i)}$) at the output of segment i was estimated from the conservative mixing of the input sources:

$$C_{exp(y,i)} = \frac{\left(C_{out(meas)(y,i-1)}Q_{out(meas)(i-1)} + \sum\left(C_{trib(meas)(y,i)}Q_{trib(meas)(i)}\right)\right)}{Q_{out(exp)(i)}} \quad \left[\text{mass volume}^{-1}\right]$$
(3)

The net in-stream retention/release efficiency of solute y at segment i ($\eta_{(y, i)}$) was calculated according to the following formula:

$$\eta_{(y,i)} = \frac{\left(C_{out(meas)(y,i)} - C_{\exp(y,i)}\right)}{\Delta A_{(i)} \times C_{\exp(i)}} \times 100 \quad \left[\% \text{km}^{-2}\right] \tag{4}$$

where $\Delta A_{(i)}$ is the river-bed area of reach i. $\eta_{(y, i)} < 0$ indicated a net retention of the solute in reach i. The opposite relationship indicated a net release. $\eta_{(y, i)}$ values were calculated for water electrical conductivity (EC), DOC and HPLC-SEC chromatograms (see below for more details). $\eta_{(y, i)}$ is independent of water flow and it can be used to compare the DOM retention/release efficiency across diverse hydrological conditions.

The dissolved organic carbon mass retention/release efficiency ($DOCr_{(i)}$) was estimated at each reach i according to the formula:

$$DOCr_{(i)} = \frac{\left(C_{out(meas)(DOC,i)} - C_{\exp(DOC,i)}\right) \times Q_{out(\exp)(i)}}{\Delta A_{(i)}} \quad \left[\text{gC s}^{-1}\,\text{km}^{-2}\right] \tag{5}$$

$DOCr_{(i)}$ was estimated only when $\eta_{(DOC, i)}$ was significantly different from zero (see below).

Sampling of lateral inputs was as comprehensive as possible and groundwater inputs were deemed unimportant in the studied system (see Section 2.4.1). However, unidentified water and solute mass inputs could not be excluded. To minimize the risk of overestimation/underestimation of the net in-stream DOM retention/release, $\eta_{(DOM, i)}$ values, were corrected using water EC values as conservative tracer (Pellerin et al., 2008). According to Eq. (4), the in-stream balance efficiency of EC ($\eta_{(EC,i)}$) was estimated at each reach i. The, $\eta_{(DOM, i)}$ values were then compared to the $\eta_{(EC,i)}$ values. Corrected $\eta_{(DOM, i)}$ values (named $\eta'_{(DOM, i)}$) were estimated according to the following criteria:

1) If both $\eta_{(DOM, i)}$ and $\eta_{(EC, i)}$ have the same sign and $|\eta_{(EC,i)}| > |\eta_{(DOM, i)}|$, then:

$$\eta'_{(DOM,i)} = 0$$

2) If both $\eta_{(DOM, i)}$ and $\eta_{(EC, i)}$ have the same sign and $|\eta_{(EC,i)}| < |\eta_{(DOM, i)}|$, then:

$$\eta'_{(DOM, i)} = \eta_{(DOM, i)} - \eta_{(EC, i)}.$$

3) If $\eta_{(DOM, i)}$ and $\eta_{(EC, i)}$ have opposite signs, then:

$$\eta'_{(DOM, i)} = \eta_{(DOM,i)}.$$

The first case describes a scenario in which the $\eta_{(DOM, i)}$ value may represent an artefact as a result of unmonitored water and solute inputs.

Following a similar procedure, for humic and protein-like balance efficiencies, two metrics were computed:

i) $\eta'_{(Hum, i)}$ and $\eta'_{(Prot, i)}$: obtained after integrating the area of the entire chromatograms;
ii) $\eta'_{(Hum, MW, i)}$ and $\eta'_{(Prot, MW, i)}$: computed at a specific molecular weight (MW) value.

The first metric ($\eta'_{(Hum, i)}$ and $\eta'_{(Prot, i)}$) provided an estimation of the retention/release efficiencies of the bulk of humic and protein-like substances. $C_{out(meas)(y,i)}$ and $C_{\exp(y,i)}$ were replaced with the observed and expected chromatogram areas ($\Sigma F_{(DOM, i)}$) obtained at the sampling site i in Eqs. (3) and (4).

The second metric ($\eta'_{(Hum, MW, i)}$ and $\eta'_{(Prot, MW, i)}$) allowed to explore the relationship between net in-stream DOM retention/release efficiencies and its apparent MW. $C_{out(meas)(y,i)}$ and $C_{exp(y,i)}$ were replaced by the observed and expected magnitudes of the chromatogram's fluorescence signal at an exact MW value in Eqs. (3) and (4). Thus, an array of $\eta'_{(Hum, MW, i)}$ and $\eta'_{(Prot, MW,i)}$ values were obtained for each reach i. Values of $\eta'_{(Hum, MW, i)}$ and $\eta'_{(Prot, MW, i)}$ were calculated in the portion of chromatograms with peaks (tails of chromatograms were omitted). The apparent MW values of humic-like chromatograms ranged from 13 to 1 kDa during drought, from 13 to 2.5 kDa during baseflow and from 13 to 5 kDa during flood. The MWs of protein-like chromatograms ranged from 12 to 0.15 kDa during drought and baseflow conditions and from 12 to 2.5 kDa during flood (Fig. A1).

2.5. Statistical analyses

Weighted average molar mass of each protein and humic-like chromatogram was estimated with two descriptors (Zhou et al., 2000): average molecular weight ($M_{w(DOM)}$) and number average molecular weight ($M_{n(DOM)}$). The $D_{DOM} = M_{w(DOM)}/M_{n(DOM)}$ ratio, which indicates the chromatogram dispersion, was also estimated:

$$M_{w(DOM)} = \frac{\sum M_j^2 N_j}{\sum M_j N_j} \tag{6}$$

$$M_{n(DOM)} = \frac{\sum M_j N_j}{\sum N_j} \tag{7}$$

where N_j is the intensity of fluorescence signal of molecular weight M_j.

DOM content differences between hydrological conditions were tested using ANOVA and Tukey post hoc analyses when data were normally distributed. Otherwise, the non-parametric Mann-Whitney-Wilcoxon test was used. Normality was tested with the Kolmogorov—Smirnov test. Variance differences between two distributions were estimated using the variance Siegel-Tukey hypothesis test. A one-sample t-test was used to determine if the net in-stream retention/release efficiencies of DOC, protein and humic-like substances ($\eta'_{(DOC)}$, $\eta'_{(Prot)}$ and $\eta'_{(Hum)}$) measured at each specific hydrological condition, were significantly different from zero. The null hypothesis was rejected at the 5% confidence level.
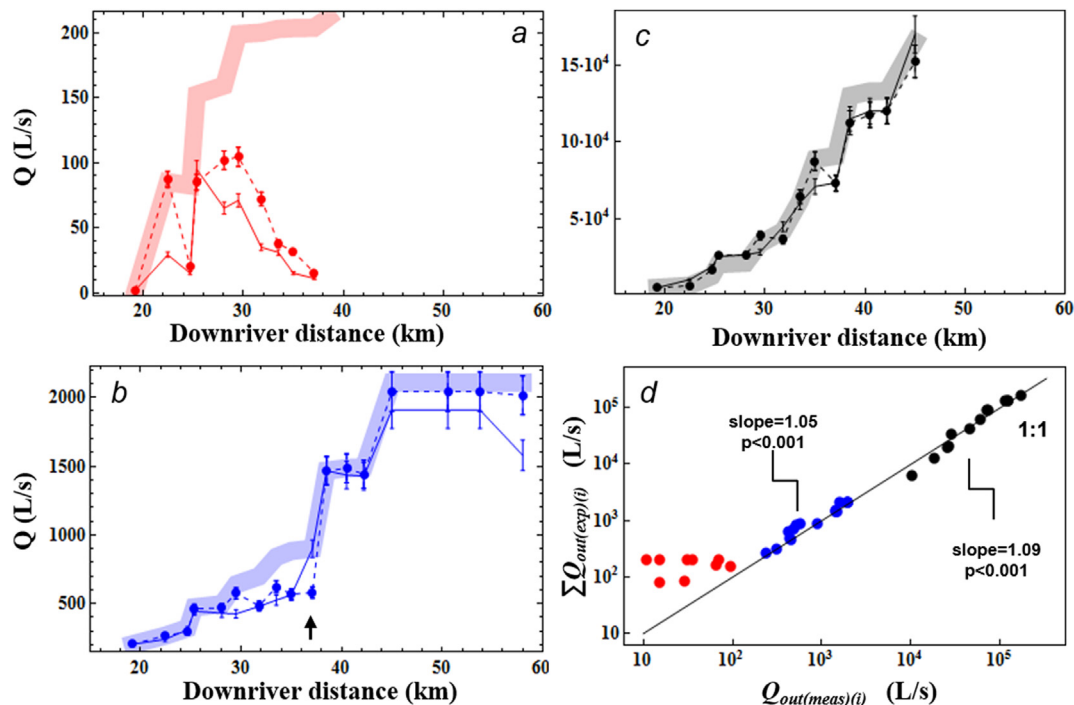
Fig. 2. Longitudinal discharge profiles during drought (panel *a*), baseflow (panel *b*) and flood (panel *c*). Solid lines show the measured discharge at the output of each fluvial segment ($Q_{out(meas)(i)}$). Bold lines show the accumulated expected discharge according the inputs from tributaries ($\sum Q_{out(exp)(i)}$). Dashed lines show the reach scale expected discharge ($Q_{out(exp)(i)}$). Error bars show the standard error of discharge measurements. In panel *b*, arrow shows the case at which $Q_{out(meas)(i)}$ is significantly larger than $Q_{out(exp)(i)}$ suggesting the input of an unknown water mass in this point of the river (see text for details). Panel d shows the relationship $\sum Q_{out(exp)(i)}$ and $Q_{out(meas)(i)}$ during the three hydrological periods. Data from baseflow (blue dots) and flood (black dots) are close to the 1:1 line, indicating that river flow is essentially governed by lateral inputs. During drought (red dots) points are located above the 1:1 line indicating remarkable water infiltration in the river channel. (For interpretation of the references to colour in this figure legend, the reader is referred to the web version of this article.)

Correlations between variables were assumed significant at the 5% level.

3. Results

3.1. Water mass balance

During drought, the discharge increased from kilometre 19 to 26 coinciding with water inputs from two WWTPs and a polluted tributary. Water flow decreased gradually downriver and disappeared from kilometre 38 (Fig. 2a). No relationship was observed between $\sum Q_{out(exp)(i)}$ and $Q_{out(meas)(i)}$ and all data plotted above the 1:1 line (Fig. 2d). Thus, the river flow was strongly attenuated by infiltration into groundwater. The discharge increased downriver during baseflow and flood conditions (Fig. 2*b* and c). The accumulated expected discharges ($\sum Q_{out(exp)(i)}$) strongly covaried ($p < 0.001$) with those measured in the field ($Q_{out(meas)(i)}$) under both hydrological conditions. Fig. 2d shows that values fitted the 1:1 line, indicating that tributary inputs governed the water flow regime in the main stem and net groundwater inputs into the river were negligible.

Although these results indicate that groundwater discharge into the river was unimportant, groundwater effluence was detected in one occasion. $Q_{out(meas)(i)}$ (900 ± 63 L/s) was visibly higher than $Q_{out(exp)(i)}$ (579 ± 42 L/s) during baseflow at kilometre 37.5 (Fig. 2*b*). Considering a standard error of 7% of the discharge measurement, approximately 22–41% of water flow that exited this reach had an unknown origin. The DOM mass balance estimated at this reach during baseflow was not taken into account in calculations because DOM composition data of groundwater were unavailable.

3.2. Electrical conductivity and DOM longitudinal profiles

The electrical conductivity (EC) increased from kilometres 20 to 28 under drought and baseflow conditions, coinciding with the direct inputs of water from two WWPTs and an anthropenically impacted tributary. The EC values stabilized downriver during baseflow with an additional minor increase at kilometre 45 after the confluence of the last major tributary. A second abrupt EC increase appeared at kilometre 40 during drought due to the input from an industrial outlet when the main stem was dry. The EC values were low during flood as consequence of substantial dilution by runoff water. A sharp increase in EC was still observable between kilometres 20 and 28, while EC values remained stable downriver (Fig. A2). The EC values estimated using the mass balance equations significantly covaried (overlapping the 1:1 line) with the observed values. The differences between the observed and predicted values were not significant (paired *t*-test, $p > 0.05$, Fig. A2). This relationship supports the hydrological evidence that river discharge is mainly governed by tributary inputs.

DOC concentrations generally increased downriver under all the three hydrological conditions (Fig. 3a). However, during flood the longitudinal increase was more gradual and smoothed. The DOC averaged (±1SD) 2.6 ± 1.7 mg/L, 1.6 ± 0.8 mg/L and 8.6 ± 2 mg/L during drought, baseflow and flood conditions respectively. DOC values during flood were significantly higher than DOC values during the other two conditions (Mann-Whitney-Wilcoxon test, $p < 0.001$). In contrast, no difference was observed between drought and baseflow values (Mann-Whitney-Wilcoxon test, $p > 0.05$).

The total fluorescence of humic-like chromatograms ($\Sigma F_{(Hum)}$, Fig. 3b) covaried with DOC ($0.74 < r^2 < 0.98$, $p < 0.01$). This
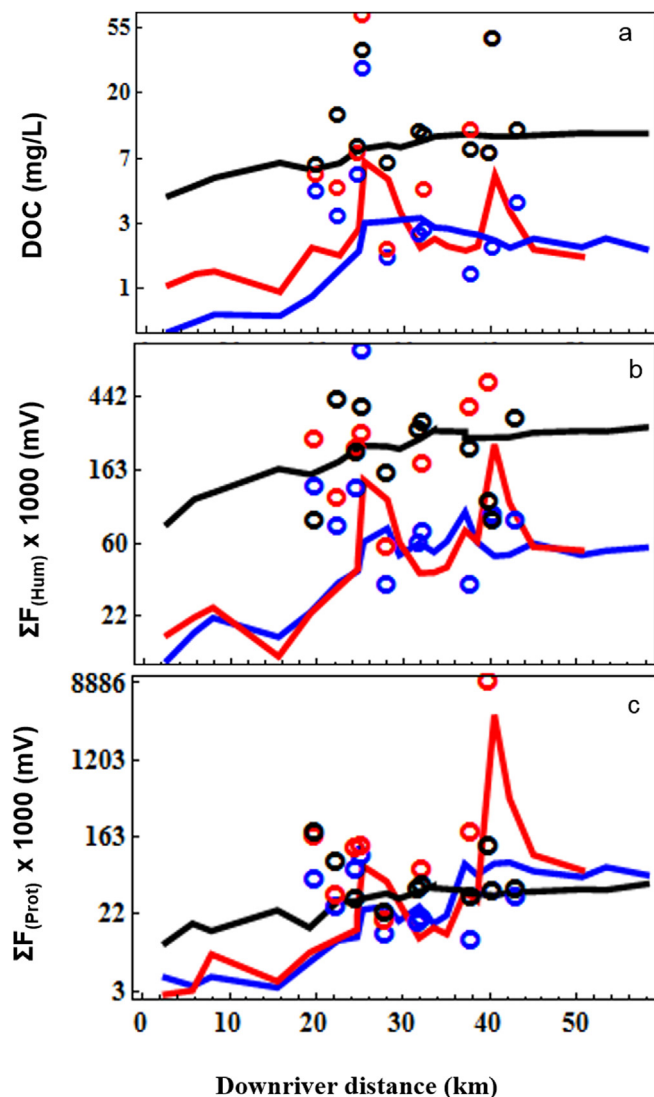
Fig. 3. Longitudinal profiles of DOC (panel a), total fluorescence of humic-like SEC chromatograms (panel b) and total fluorescence of protein-like SEC chromatograms (panel c). Blue, red and black correspond to the baseflow, drought and flood conditions respectively. Solid lines are the main stem. Circles are the tributaries. Vertical axes are log transformed for a visual purpose. (For interpretation of the references to colour in this figure legend, the reader is referred to the web version of this article.)
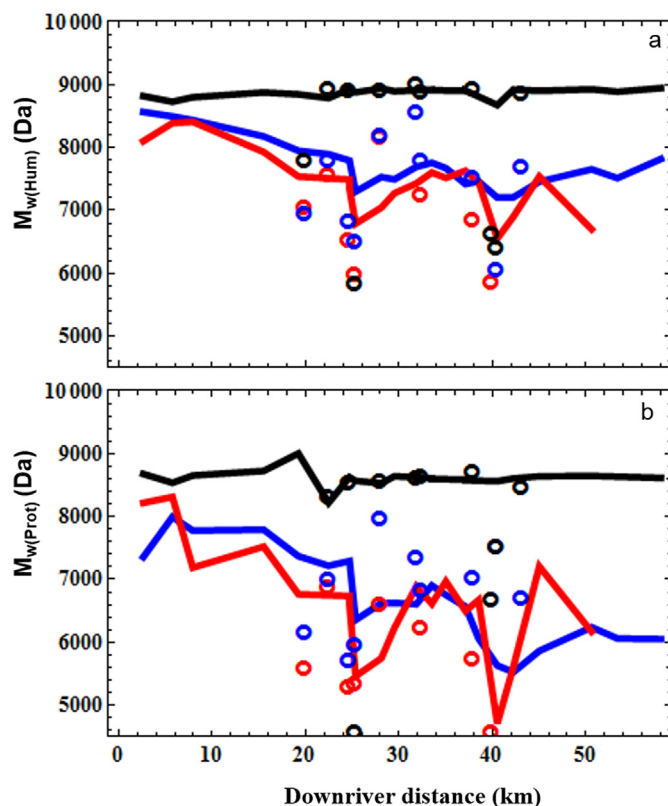

Fig. 4. Longitudinal profiles of humic-like (panel a) and protein-like (panel b) weighted averaged molecular weight (M_w). Symbols are the same as in Fig. 3.

relationship was also significant for $\Sigma F_{(Prot)}$ (Fig. 3c) during flood condition ($r^2 = 0.91$, $p < 0.01$), but not during baseflow and drought conditions ($r^2 < 0.23$, $p > 0.05$).

Protein and humic-like molecular weight distributions exhibited significantly larger $M_{w(DOM)}$ and $M_{n(DOM)}$ values and lower $D_{(DOM)}$ (Table 2) during flood condition (ANOVA and Tukey post hoc test, $p < 0.001$). The $M_{w(Prot)}$, $M_{w(Hum)}$, $M_{n(Prot)}$ and $M_{n\ (Hum)}$ values

significantly decreased downriver under baseflow ($r^2 > 0.53$, d.f. = 19, $p < 0.01$) and drought ($r^2 > 0.49$, d.f. = 17, $p < 0.01$) conditions, but not during flood condition (Fig. 4). The longitudinal decrease of $M_{n(Prot)}$ values was steeper than that of $M_{n(Hum)}$ values.

The humic and protein-like chromatograms strongly varied, particularly under different hydrological conditions (Fig. A1). The humic-like chromatograms displayed a unimodal log tailed distribution with a peak located between 7 and 13 kDa. Some smaller molecules (up to 1 kDa) appeared during baseflow and drought conditions, but not during flood conditions. In contrast the protein-like chromatograms showed multi-peak shapes. The peaks were widely distributed along the entire molecular spectra during drought and baseflow conditions but exhibited a unimodal long tailed distribution under flood conditions.

3.3. Net in-stream DOM retention/release efficiencies

Net in-stream retention/release efficiencies ($\eta'_{(DOM)}$) of DOC, protein and humic-like substances averaged (± 1SD) -19.3 ± 19.9, 41.3 ± 28 and -33 ± 32 respectively during drought conditions.

Table 2
Average $\pm$ SD values of average molecular weight ($M_{w(DOM)}$), average molecular weight number ($M_{n(DOM)}$) and polydispersity ($D_{(DOM)}$) for humic and protein-like substances under baseflow, drought and flood respectively.

	Humic-like			Protein-like		
	$M_{w(DOM)}$ (kDa)	$M_{n(DOM)}$ (kDa)	$D_{(DOM)}$	$M_{w(DOM)}$ (kDa)	$M_{n(DOM)}$ (kDa)	$D_{(DOM)}$
Drought	7.5 ± 0.5	6.1 ± 0.6	1.2 ± 0.03	6.6 ± 0.9	4.2 ± 1.4	1.7 ± 0.4
Baseflow	7.7 ± 0.4	6.4 ± 0.5	1.2 ± 0.04	6.7 ± 0.7	4.2 ± 1.3	1.7 ± 0.5
Flood [a]	8.9 ± 0.07	7.8 ± 0.2	1.1 ± 0.03	8.6 ± 0.1	7.3 ± 0.5	1.2 ± 0.07

[a] Denotes significant difference with respect to the other hydrological conditions (ANOVA and Tukey post hoc test, $p < 0.01$).

Retentions were statistically significant (t $<$ -2.74, d.f. = 7, p $<$ 0.05). $\eta'_{(DOM)}$ strongly decreased during baseflow and retention remained significant for DOC ($\eta'_{(DOC)}$ = -2.7 ± 4.9, t = -2.23,d.f. = 14, p $<$ 0.05) but not for protein and humic-like substances (t $>$ -2.1, d.f. = 14, p $>$ 0.05). None of the DOM efficiency values significantly differed from zero during flood conditions (t $>$ -1.4, d.f. = 12, p $>$ 0.05).

The absolute carbon mass net retention, $DOCr_{(i)}$, averaged -7.6 ± 11 and -6 ± 11 gC s^{-1} km^{-2} during drought and baseflow conditions, respectively. Approximately 40% of inputs were retained within the system during drought conditions based on a total tributary DOC input of 1.7 g C/s. The estimated DOC inputs from tributaries were 5.95 gC/s, and approximately 30% of these inputs were retained within the system during baseflow conditions.

Combining the three hydrological episodes, $\eta'_{(DOC)}$ covaried with that of $\eta'_{(Prot)}$ (r^2 = 0.5, d.f. = 32, p $<$ 0.001) and $\eta'_{(Hum)}$ (r^2 = 0.33, d.f. = 32, p $<$ 0.001). Additionally, $\eta'_{(Hum)}$ and $\eta'_{(Prot)}$ displayed a correlated relationship (r^2 = 0.69, d.f. = 32, p $<$ 0.001). The highest DOM retention values (i.e. $\eta'_{(DOM)} < 0$) were typically estimated at the upriver reaches during drought and baseflow conditions (Fig. 5). However, $\eta'_{(DOC)}$, $\eta'_{(Prot)}$ and $\eta'_{(Hum)}$ values were unrelated to the downriver distance ($r^2 < 0.24$, p$>$0.05).

The $\eta'_{(Hum, MW)}$ and $\eta'_{(Prot, MW)}$ values were highly variable. The distributions of both $\eta'_{(Prot, MW)}$ and $\eta'_{(Hum, MW)}$ were bimodal during drought (Fig. 6a$_3$), with median values of -38%/km^2 and -28.2%/km^2, respectively. The difference among median values was significant (Mann-Whitney-Wilcoxon test, p $<$ 0.05), while variances were statistically similar (variance Siegel-Tukey hypothesis test, p $>$ 0.05). Both $\eta'_{(Prot, MW)}$ and $\eta'_{(Hum, MW)}$ data were distributed according to an unimodal distribution during baseflow condition, with median values close to zero (-4.8%/km^2 and -3.5%/km^2 respectively, Fig. 6b$_3$). No difference was observed between the two median values (Mann-Whitney-Wilcoxon test, p $>$ 0.05). However, the $\eta'_{(Prot, MW)}$ variance was significantly larger than that of humic-like moieties (variance Siegel-Tukey hypothesis test, p $<$ 0.001). Both $\eta'_{(Prot, MW)}$ and $\eta'_{(Hum, MW)}$ median values were close to zero (-0.1 and -0.05%/km^2 respectively) during flood condition. The distributions displayed non-significant differences in median and variance (Mann-Whitney-Wilcoxon test, p $>$ 0.05 and variance Siegel-Tukey hypothesis test, p $>$ 0.05, Fig. 6c$_3$).

Retention of humic and protein-like moieties during drought was slightly larger at low molecular weights. Thus, median values of $\eta'_{(Hum, MW)}$ and $\eta'_{(Prot, MW)}$ were significantly positively related to the molecular weights (humic: r^2 = 0.39, d.f. = 39, p $<$ 0.01, protein: r^2 = 0.46, d.f. = 74, p $<$ 0.01, Fig. 6a$_1$,a$_2$). This trend was also
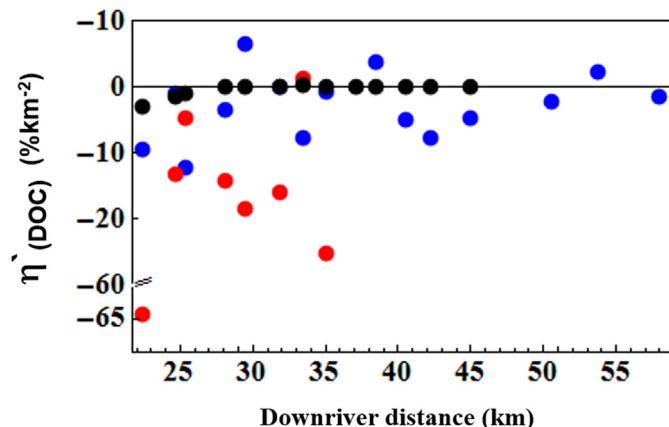
discernible for humic substances during baseflow condition (r^2 = 0.74, d.f. = 26, p $<$ 0.01, Fig. 5b$_1$,b$_2$). During flood, humic and protein-like substances behaved conservatively along the entire MW spectra (Fig. 6c$_1$,c$_2$).

Fig. 7 illustrates the $\eta'_{(Hum, MW)}$ and $\eta'_{(Prot, MW)}$ distribution values across the entire molecular weight spectra and along the fluvial continuum, during baseflow and drought conditions. The retention of humic and protein-like substances was distributed throughout the 16 km fluvial segment during drought, but largest retention occurred at the initial reaches (between kilometres 22 and 27, Fig. 7a and c). High DOM retention (both humic and protein-like) attenuated DOC concentrations in the fluvial system in spite of lateral inputs with elevated DOC concentrations. For instance, the large DOC inputs from a WWTP and an industrial outlet at kilometres 25 and 26 were partially damped after six kilometres. However, release of small protein-like substances ($<$1 kDa) occurred after kilometre 30 in a portion of the river that received little anthropogenic inputs.

The analysis of the spatial variability of net DOM retention/release efficiencies was more complete during baseflow conditions because measurements encompassed 39 km of the main stem. Humic-like moiety behaved almost conservatively along the majority of the river reach (Fig. 7b). In contrast, processing of protein-like compounds appeared spatially variable and molecules smaller than 1 kDa appeared highly reactive. These small DOM fractions shifted from net retention ($\eta'_{(Prot, MW)} < 0$) at the upper reaches, coinciding with the first major anthropogenic inputs, to a net release ($\eta'_{(Prot, MW)} > 0$) in a large reach (from kilometres 32 to 42), when the river received inputs from streams with relatively minimal anthropogenic influences. These fractions were only weakly retained downriver (from kilometre 45 to the river mouth), where there no major tributaries exist. In contrast, protein-like molecules larger than 1 kDa were typically less reactive with sporadic retention and release in the fluvial system (Fig. 7d).

4. Discussion

The study of how the structure and size of rivers networks influence their biogeochemical processes is a fertile and challenging research topic (McClain et al., 2003; Fisher et al., 2004; Vidon et al., 2010). Within the umbrella of the river continuum and spiralling concepts (Vannote et al., 1980; Newbold et al., 1981), meta-analyses of hundreds of reach-scale mass balance studies performed during the last 30 years in streams/rivers around the world, allow us to understand if and how river size controls inorganic solutes retention (Ensign and Doyle, 2006; Wollheim et al., 2006). However, comparable knowledge regarding DOM processing is currently lacking. This knowledge gap evidences the need to expand in situ DOM balance measurements worldwide.

4.1. DOM properties and retention along the river continuum

In the Tordera river, DOC increased downriver during flood conditions. Meanwhile, DOM properties ($M_{w(DOM)}$, $M_{n(DOM)}$ and $D_{(DOM)}$ of humic and protein-like substances) and retention/release efficiencies ($\eta'_{(DOC)}$, $\eta'_{(Prot, MW)}$ and $\eta'_{(Hum, MW)}$) were stable along the main reach. In addition, values of $\eta'_{(DOC)}$, $\eta'_{(Prot, MW)}$ and $\eta'_{(Hum, MW)}$ were close to zero. Thus, the entire river acted as a homogeneous passive corridor for DOM transport during flood. This result was expected as water travelled the entire main segment in 11 h and solutes had little chance to interact with river bed biota. Ex situ bioassay experiments showed that DOM collected during storm episodes is potentially bioavailable for microbiota (Buffam et al., 2001; McLaughlin and Kaplan, 2013). Therefore, although floods inhibit in-stream DOM processing, they may stimulate the
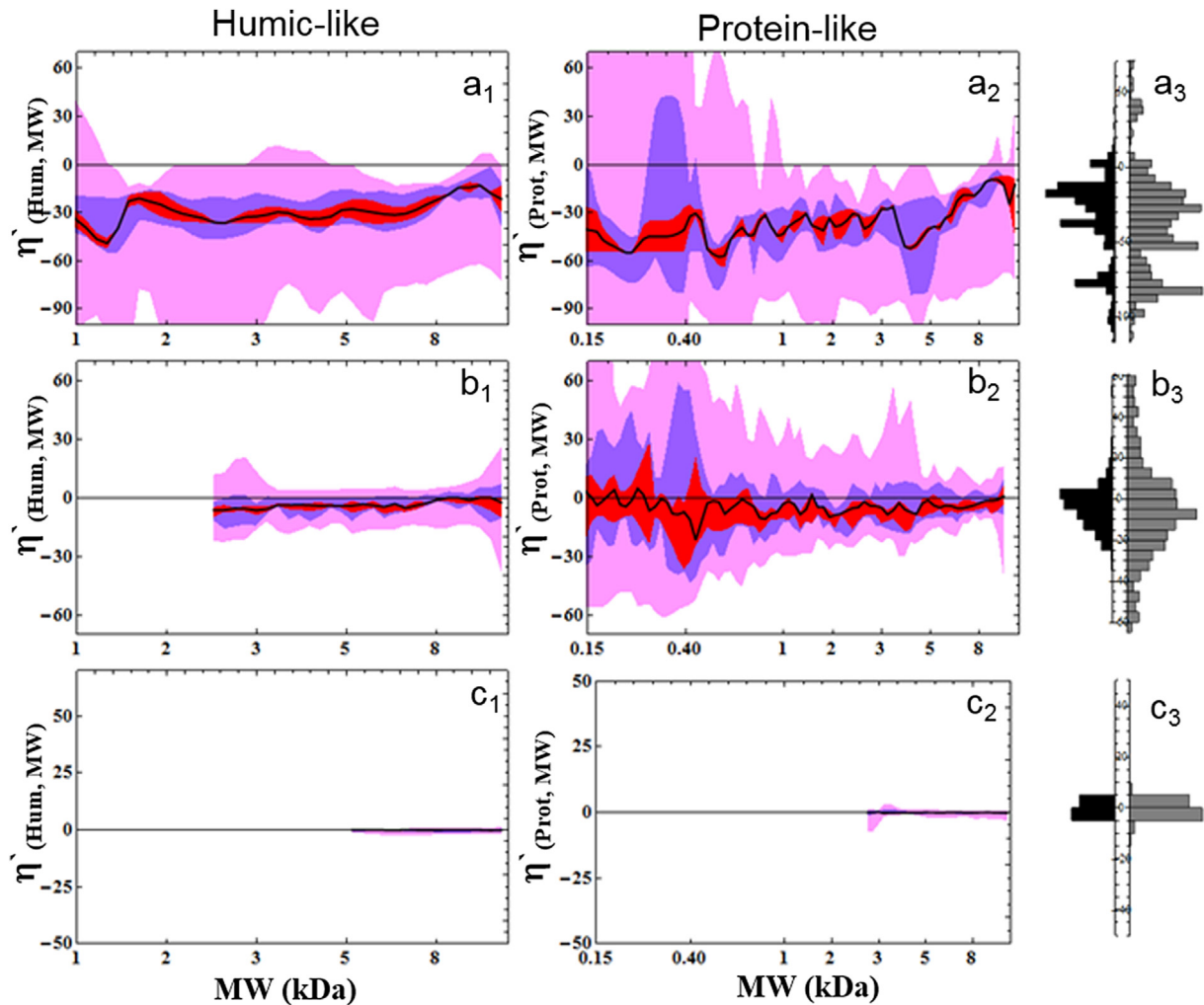
Fig. 5. Longitudinal profiles of DOC $\eta'_{(DOC, i)}$ Colors of dots are the same as in Fig. 3.

Fig. 6. Changes of the humic and protein-like in-stream net balance rates ($\eta'_{(Hum, MW)}$, left panels and $\eta'_{(Prot, MW)}$, right panels) across the entire molecular weight range during the three hydrological episodes. Panels a_1 and a_2 refer to drought; b_1 and b_2, to baseflow; c_1 and c_2 to the flood. Solid black lines indicate the median values. Solid color areas delimitate the percentiles ranges. Pink area delimitates the 90th and 10th percentiles. Purple area the 70th and 30th percentiles. The red area are the 60th and 40th percentiles. Paired histograms on the right (a_3, b_3 and c_3) compare the distribution of $\eta'_{(Hum, MW)}$ (black bars) and $\eta'_{(Prot, MW)}$ (gray bars) values. (For interpretation of the references to colour in this figure legend, the reader is referred to the web version of this article.)

microbial activity in downriver environments that receive these DOM inputs, such as lakes or deltaic ecosystems (Palmer et al., 2015).

In contrast, DOC concentration clearly increased downriver and exhibited large oscillations under baseflow and drought conditions. $M_{w(Hum)}$ and $M_{w(Prot)}$ values decreased downriver and $\eta'_{(DOC)}$, $\eta'_{(Prot, MW)}$ and $\eta'_{(Hum, MW)}$ were highly variable. Furthermore, differences in $M_{w(Hum)}$ and $M_{w(Prot)}$ values between drought (or baseflow) and flood conditions increased downriver (Fig. 4). Therefore, in terms of DOM composition, downriver sites were more sensitive to discharge changes than upstream sites. These findings are opposite to those obtained from meta-analyses of large DOM data set from US rivers/streams (Creed et al., 2015). This divergence suggests that stable DOM concentrations do not exclude shifts in DOM composition.

$DOCr$ ranged between −33.7 and 9.7 gC s^{-1} km^{-2} (−2.9–0.8 gC day^{-1} m^{-2}) during drought and baseflow conditions, respectively. This range falls within that reported by Sirivichi et al. (2011) and Kaushal et al. (2014) in rivers for baseflow conditions. Little is known about the net DOC retention magnitude in rivers

over an entire hydrological year. By knowing the approximate contribution of drought, baseflow, and flood conditions to the annual water flow and, assuming that the three sampling campaigns are representative of DOC loads from tributaries, then approximately 9, 101 and 193 kgC of DOC enter into the main stem during drought, baseflow, and flood conditions each year. According to our estimates, the main stem retained approximately 40%, 30% and 0% of the DOC input during drought, baseflow and flood conditions, respectively. Therefore, the river retains roughly 10% of the total annual DOC that enters into the system. This estimation suggests that the Tordera behaves more as a passive pipe than a reactor on an annual scale. This conclusion is similar to those obtained by combining *ex situ* incubations and DOC flows in a temperate river (del Giorgio and Pace, 2008), surveys in small peat streams (Stutter et al., 2013; Palmer et al., 2015) and sampling under baseflow in a temperate river (Wollheim et al., 2015) but considerably lower than the 48−69% suggested in a modelling study of a northern England river (Moody et al., 2013).

In contrast to DOM concentrations and properties, net in-stream DOM retention/release efficiencies did not exhibit longitudinal
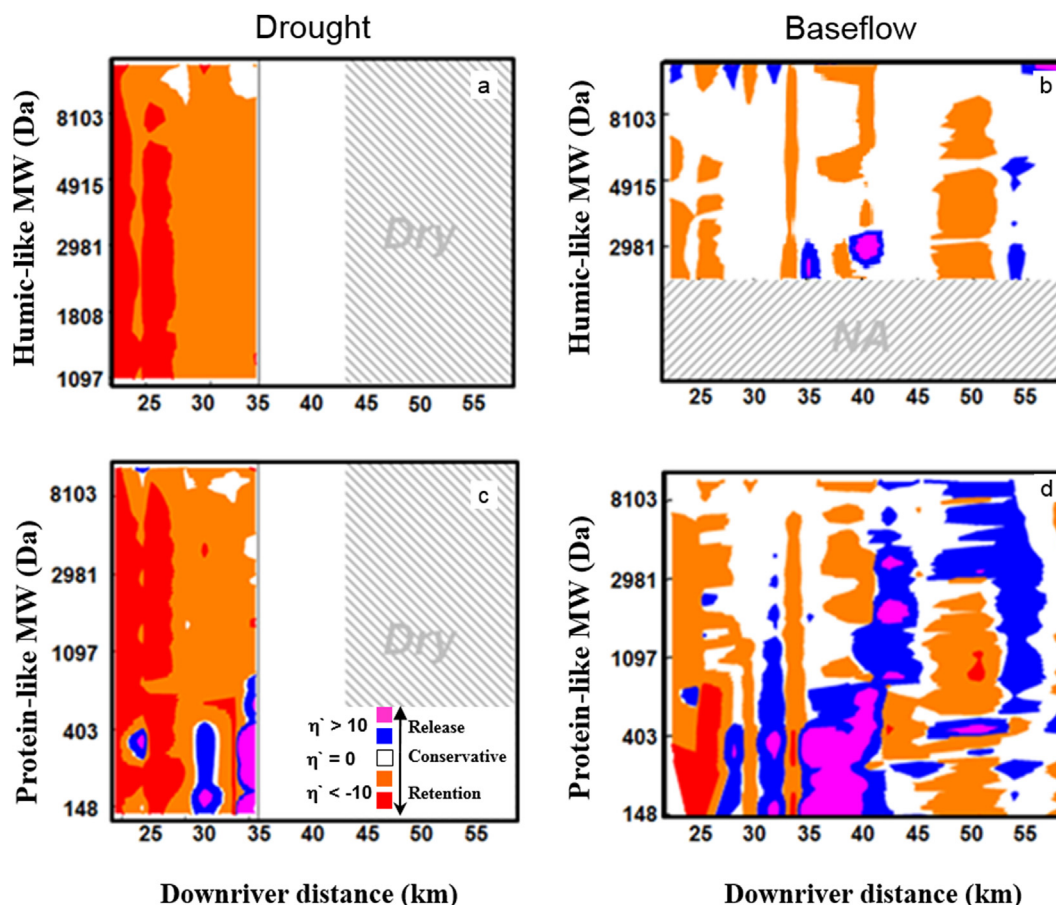
Fig. 7. Contour plots illustrating the response of the humic-like (upper panels *a* and *b*) and protein-like (lower panels *c* and *d*) η′ rates changes across the molecular weight spectra and along the fluvial continuum during baseflow (panel *a* and *c*) and drought conditions (panels *b* and *d*). Red and orange colors indicate negative η′ rates (i.e. net retention). Blue and magenta colors indicate positive η′ rates (i.e. net release). White color indicate nil η′ rates (i.e. conservative). (For interpretation of the references to colour in this figure legend, the reader is referred to the web version of this article.)

patterns. This result is similar to that reported for DOC by Sirivichi et al. (2011) and Kaushal et al. (2014). However, differences were observed between drought and baseflow. The entire river efficiently retained DOC and humic and protein-like substances during drought. In contrast, net retention efficiencies of protein and humic-like substances were much lower and showed a manifest spatial heterogeneity during baseflow. Specifically, the small protein-like fraction (<1 kDa) was retained in the upstream reaches, released in the middle part and feebly retained (or "semi-labile", Kaplan et al., 2008) in the downriver reaches. The *in situ* production of small protein-like molecules in the middle reaches could be related to the release of small autochthonous DOM molecules from microbiota (Romera-Castillo et al., 2010; Fasching et al., 2014) or plant exudates (Elliott et al., 2006). However, the retention of these molecules was minimal in the subsequent river reaches, suggesting that this fraction was not readily available to the microbiota under baseflow conditions.

4.2. DOM net retention. Are molecular properties important?

Net retention of both humic and protein-like molecules were strongly enhanced under drought conditions. Humic substances are commonly associated to a more resistant DOM pool (Kelleher and Simpson, 2006) and proteins to a more labile DOM pool (Cory and Kaplan, 2012; Hosen et al., 2014). Our estimates confirm that protein-like substances are more retained than humic substances.

Nevertheless, this finding also supports the evidence that humic substances are not exempt to degradation (Covert and Moran, 2001; Seitzinger et al., 2005; Singer et al., 2012; Fasching et al., 2014). Additionally, a link between net retention of humic and protein-like moieties and their molecular weight emerged under drought condition. Though this preference for small substances was subtle it suggests that small molecules are more reactive than the larger molecules and agrees with the results from Covert and Moran (2001) and Berggren et al. (2010) and refutes the SRC model (Amon and Benner, 1996). In any case, these results evidence that *in situ* DOM selective retention (humic vs. protein or large vs. small molecules) appears strongly linked to the hydrological conditions of the studied system. This finding does not minimize the relevance of the DOM molecular structure to its reactivity. However, it supports the idea that environmental factors mediate the importance of molecular structure on organic carbon lability (Marín-Spiotta et al., 2014). It is important to remark that DOM bioavailability is typically inferred from *ex situ* laboratory incubations that inevitably reset the relevance of hydrology. Therefore, the present study highlights the importance of hydrological fluctuations on DOM transport and fate. This information represents a step forward to obtain more realistic estimates of DOM processing rates and provides a necessary step to establish a connection between small-scale laboratory bioassay experiments and large-scale measurements.

5. Conclusions

This study quantified the *in situ* net DOC, protein and humic-like moieties retention/release along a Mediterranean river under drought, baseflow and flood conditions.

- DOC mass balances revealed that the river switched from a highly retentive system during drought condition to a passive pipe during flood conditions.
- Drought condition promotes DOM retention in the system. The protein-like moieties were significantly more retained than the humic-like moieties. However, the humic-like substances were not exempt to degradation. Additionally, the humic and protein-like substances retention efficiencies increased at low apparent molecular weight.
- From a longitudinal perspective, the entire fluvial corridor contributed to DOC and humic and protein-like moieties net retention during drought. In contrast, net retention/release efficiencies exhibited spatial variability during baseflow. Specifically, small-sized protein-like moieties (<1 kDa) were retained in the upper reaches, released in the middle, and only weakly retained in the downriver reaches.

- Based on these results, the Tordera river retains approximately 10% of total DOC mass that flows into the system each year, suggesting that the river behaves more as a passive pipe than as a reactor.
- This research stresses the importance of expanding our observations beyond baseflow conditions to extreme hydrological episodes, to quantify the impact of fluvial corridors on DOM fate and transport.
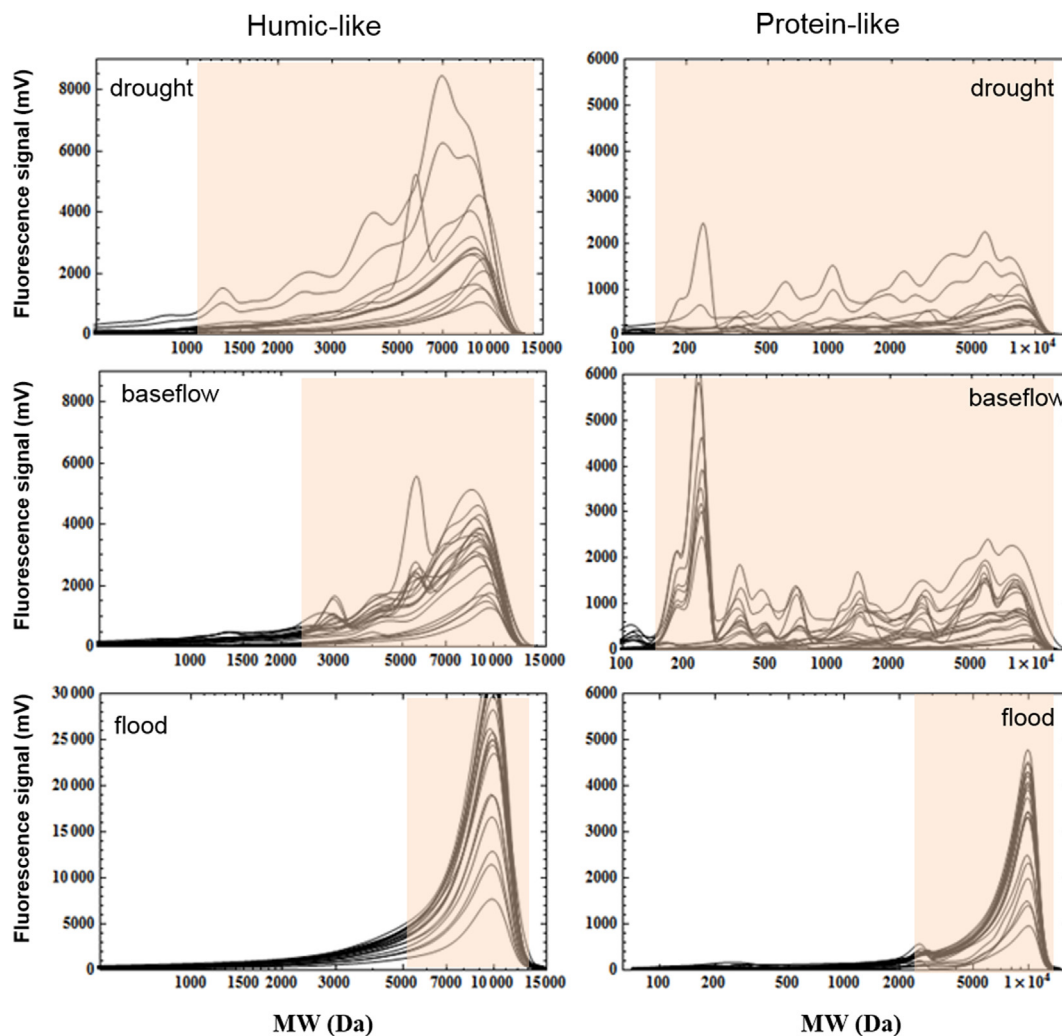
Appendix

Fig. A1. Humic and protein-like SEC chromatograms obtained during the three hydrological conditions in each sampling site. The shaded pink windows show the molecular weight interval considered for mass balance estimations (see text, for details).
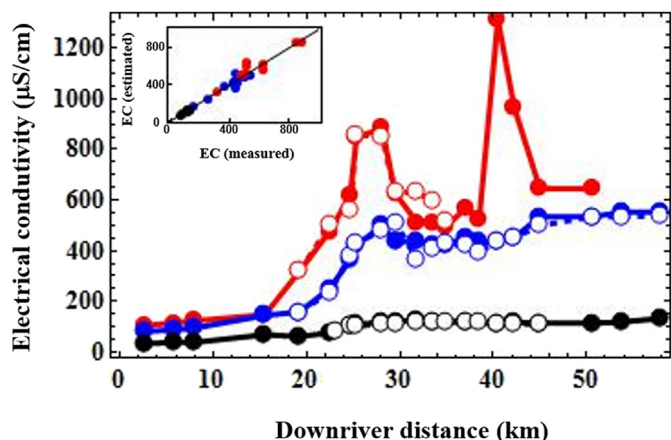
Fig. A2. Longitudinal profiles of measured and estimated electrical conductivity along the main stem. Blue, red and black dots correspond to the baseflow, drought and flood samplings respectively. Open dots are the estimated electrical conductivity (EC) values according the mass balance. The inset shows the relationship between the measured and the estimated EC values (units are mS/cm). Solid line shows the 1:1 line.

References

Allpike, B.P., Heitz, A., Joll, C.A., Kagi, R.I., Abbt-braun, G., Frimmel, F.H., Brinkmann, T., Her, N., Amy, G., 2005. Size exclusion chromatography to characterize DOC removal in drinking water treatment. Environ. Sci. Technol. 37, 2334–2342.

Amon, R.M.W., Benner, R., 1996. Bacterial utilization of different size classes of dissolved organic matter. Limnol. Oceanogr. 41, 41–51.

Attermeyer, K., Hornick, T., Kayler, Z.E., Bahr, A., Zwirnmann, E., Grossart, H.P., Premke, K., 2014. Enhanced bacterial decomposition with increasing addition of autochthonous to allochthonous carbon without any effect on bacterial community composition. Biogeosciences 11, 1479–1489.

Battin, T.J., Kaplan, L.A., Findlay, S., Hopkinson, C.S., Martí, E., Packman, C.S., Newbold, J.D., Sabater, F., 2009. Biophysical controls on organic carbon fluxes in fluvial networks. Nat. Geosci. 1, 95–100.

Berggren, M., Laudon, H., Haei, M., Strom, L., Jansson, M., 2010. Efficient aquatic bacterial metabolism of dissolved low-molecular-weight compounds from terrestrial sources. ISME 4, 408–416.

Bertilsson, S., Tranvik, L.J., 2000. Photochemical transformation of dissolved organic matter in lakes. Limnol. Oceanogr. 45, 753–762.

Buffam, I., Galloway, J.N., Blum, L.K., McGlathery, K.J., 2001. A stormflow/baseflow comparison of dissolved organic matter concentrations and bioavailability in an Appalachian stream. Biogeochemistry 53, 269–306.

Bodhipaksha, L.C., Sharpless, C.M., Chin, Y.P., Sander, M., Langston, W.K., MacKay, A.A., 2015. Triplet photochemistry of effluent and natural organic matter in whole water and isolates from effluent-receiving rivers. Environ. Sci. Technol. 49, 3453–3463.

Chanson, H., 2004. The Hydraulics of Open Channel Flow, second ed. Butterworth-Heinemann, Oxford, UK, p. 630.

Chow, V.T., 1959. Open-channel Hydraulics. McGraw-Hill, New York, p. 680.

Coble, P.G., 1996. Characterization of marine and terrestrial DOM in seawater using excitation emission matrix spectroscopy. Mar. Chem. 51, 325–346.

Cory, R.M., Kaplan, L.A., 2012. Biological lability of streamwater fluorescent dissolved organic matter. Limnol. Oceanogr. 57, 1347–1360.

Covert, J.S., Moran, M.A., 2001. Molecular characterization of estuarine bacterial communities that use high- and low-molecular weight fractions of dissolved organic carbon. Aquat. Microb. Ecol. 25 (2), 127–139.

Creed, I.F., et al., 2015. The river as a chemostat: fresh perspectives on dissolved organic matter flowing down the river continuum. Can. J. Fish. Aquat. Sci. http://dx.doi.org/10.1139/cjfas-2014-0400.

del Giorgio, P.A., Pace, M.L., 2008. Relative Independence of dissolved organic carbon transport and processing in a large temperate river: the Hudson river as bot pipe and reactor. Limnol. Oceanogr. 53, 185–197.

Di Baldassarre, G., Montanari, A., 2009. Uncertainty in river discharge observations: a quantitative analysis. Hydrol. Earth Syst. Sci. 13, 913–921.

Emerson, D.G., Vecchia, A.V., Dahl, A.L., 2005. Evaluation of Drainage-area Ratio Method Used to Estimate Streamflow for the Red River of the North Basin, North Dakota and Minnesota. Scientific Investigations Report 2005-5017. U.S. Department of the Interior and U.S. Geological Survey.

Ejarque-Gonzalez, E., Butturini, A., 2014. Self-organising maps and correlation analysis as a tool to explore patterns in excitation-emission matrix data sets and to discriminate dissolved organic matter components. PLoS One 9 (6), e99618.

Elliott, S., Lead, J.R., Baker, A., 2006. Characterization of the fluorescence from freshwater, planktonic bacteria. Water Res. 40, 2075–2083.

Ensign, S.H., Doyle, M.W., 2006. Nutrient spiraling in streams and river networks.

J. Geophys. Res. 111, G04009. http://dx.doi.org/10.1029/2005JG00011.

Fasching, C., Behounek, B., Singer, G.A., Battin, T.J., 2014. Microbial degradation of terrigenous dissolved organic matter and potential consequences for carbon cycling in brown-water streams. Sci. Rep. 4, 4981. http://dx.doi.org/10.1038/srep04981.

Fasching, C., Ulseth, A.J., Behounek, B., Schelker, J., Steniczka, G., Battin, T.J., 2015. Hydrology controls dissolved organic matter export and composition in an Alpine stream and its hyporheic zone. Limnol. Oceanogr. http://dx.doi.org/10.1002/lno.10232.

Fellman, J.B., Spencer, R.G.M., Raymon, P.A., Pettit, N.E., Skrzypek, G., Hernes, P.J., Grierson, P., 2014. Dissolved organic carbon biolability decreases along its modernization in fluvial networks in an ancient landscape. Ecology 95, 2622–2632.

Findlay, S., 2010. Stream microbial ecology. J. North Am. Benthol. Soc. 29, 170–181.

Fischer, H., Sachse, A., Steinberg, C.E.W., Pusch, M., 2002. Differential retention and utilization of dissolved organic carbon by bacteria in river sediments. Limnol. Oceanogr. 47, 1702–1711.

Fisher, S.G., Sponseller, R.A., Heffernan, J.B., 2004. Horizons in stream biogeochemistry: flowpaths to progress. Ecology 85, 2369–2379.

Gonsior, M., Peake, B.M., Cooper, W.T., Podgorski, D., D'Andrilli, J., Cooper, W.J., 2009. Photochemically induced changes in dissolved organic matter identified by ultrahigh resolution fourier transform ion cyclotron resonance mass spectrometry. Environ. Sci. Technol. 43, 698–703.

Gordon, E.S., Goni, M.A., 2003. Sources and distribution of terrigenous organic matter delivered by the Atchafalaya river to sediments in the northern Gulf of Mexico. Geochim. Cosmochim. Acta 67, 2359–2375.

Grayson, R.C., Gippel, C.J., Finlayson, B.L., Hart, B.T., 1997. Catchment-wide impacts on water quality: the use of 'snapshot' sampling during stable flow. J. Hydrol. 199, 121–134.

Her, N., Amy, G., McKnight, D., Sohn, J., Yoon, Y., 2003. Characterization of DOM as function of MW by fluorescence EEM and HPLC-SEC using UVA, DOC and fluorescence detection. Water Res. 37, 4295–4303.

Hosen, J.D., McDonough, O.T., Febria, C.M., Palmer, M.A., 2014. Dissolved organic matter quality and bioavailability changes across an urbanization gradient in headwater streams. Environ. Sci. Technol. 48, 7817–7824.

Kaplan, L.A., Wiegner, T.N., Newbold, J.D., Ostrom, P.H., Gandhi, H., 2008. Untangling the complex issue of dissolved organic carbon uptake: a stable isotope approach. Freshw. Biol. 53, 855–864.

Kaushal, S.S., Newcomb, K.D., Findlay, S.E.G., Newcomer Johnson, T., Duan, S., 2014. Longitudinal patterns in carbon and nitrogen fluxes and upstream metabolism along an urban watershed continuum. Biogeochemistry 121, 23–44.

Kelleher, B.P., Simpson, A.J., 2006. Humic substances in soils: are they really chemically distinct? Environ. Sci. Technol. 40, 4605–4611.

Marín-Spiotta, E., Gruley, K.E., Crawford, J., Atkinson, E.E., Miesel, J.R., Greene, S., Cardona-Correa, C., Spencer, R.G.M., 2014. Paradigm shifts in soil organic matter research affect interpretations of aquatic carbon cycling: transcending disciplinary and ecosystem boundaries. Biogeochemistry 117, 279–297.

Marschner, B., Kalbitz, K., 2003. Control of bioavailability and biodegradability of dissolved organic matter in soils. Geoderma 113, 211–235.

Mas-Pla, J., Menció, A., 2009. Water indicators applied to biodiversity monitoring on the Tordera river. In: V Trobada d'estudiosos dels Parcs de la Serralada Litoral Central. Diputació de Barcelona, pp. 157–167.

McClain, M.E., et al., 2003. Biogeochemical hot spots and hot moments at the interface of terrestrial and aquatic ecosystems. Ecosystems 6, 301–312.

McLaughlin, C., Kaplan, L.A., 2013. Biological lability of dissolved organic carbon in stream water and contributing terrestrial sources. Freshw. Sci. 32, 1219–1230.

Meng, F., Huang, G., Yang, X., Li, Z., Li, J., Cao, J., Wang, Z., Sun, Li, 2013. Identifying the sources and fate of anthropogenically impacted dissolved organic matter (DOM) in urbanized rivers. Water Res. 47, 5027–5039.

Miller, W.L., Zepp, R.G., 1995. Photochemical production of dissolved inorganic carbon from terrestrial organic-matter significance to the oceanic organic carbon cycle. Geophys. Res. Lett. 22, 417–420.

Moody, C.S., Worrall, F., Evans, C.D., Jones, T.G., 2013. The rate of loss of dissolved organic carbon (DOC) through a catchment. J. Hydrol. 492, 139–150.

Nebbioso, A., Piccolo, A., 2013. Molecular characterization of dissolved organic matter (DOM): a critical review. Anal. Bioanal. Chem. 405, 109–124.

Newbold, J.D., Elwood, J.W., O'Neill, R.V., Van Winkle, W., 1981. Measuring nutrient spiralling in streams. Can. J. Fish. Aquat. Sci. 38, 860–863.

Palmer, S.M., Evans, C.D., Chapman, P.J., Burden, A., Jones, T.J., Allott, T.E.H., Evans, M.G., Moody, C.S., Worrall, F., Holden, J., 2015. Sporadic hotspots for physico-chemical retention of aquatic organic carbon: from peatland headwater source to sea. J. Aquat. Sci. http://dx.doi.org/10.1007/s00027-015-0448-x.

Pellerin, B.A., Wollheim, W.M., Feng, X., Vorosmarty, C.J., 2008. The application of electrical conductivity as a tracer for hydrograph separation in urban catchments. Hydrol. Process 22, 1810–1818.

Raymond, P.A., Saiers, J.E., 2010. Event controlled DOC export from forested watersheds. Biogeochemistry 100, 197–209.

Romaní, A.M., Amalfitano, S., Artigas, J., Fazi, S., Sabater, S., Timoner, X., Ylla, I., Zoppini, A., 2012. Microbial biofilm structure and organic matter use in Mediterranean streams. Hydrobiologia 719, 43–58.

Romera-Castillo, C., Chen, M.L., Yamashita, Y., Jaffe, R., 2014. Fluorescence characteristics of size-fractionated dissolved organic matter: implications for a molecular assembly based structure? Water Res. 55, 40–51.

Romera-Castillo, C., Sarmento, H., Alvarez-Salgado, X.A., Gasol, J.M., Marrase, C., 2010. Production of chromophoric dissolved organic matter by marine

phytoplankton. Limnol. Oceanogr. 55, 446—454.

Seitzinger, S.P., Hartnett, H., Lauck, R., Mazurek, M., Minegishi, T., Spyres, G., Styles, R., 2005. Molecular-level chemical characterization and bioavailability of dissolved organic matter in stream water using electrospray-ionization mass spectrometry. Limnol. Oceanogr. 50, 1—12.

Singer, G.A., Fasching, C., Wilhelm, L., Niggemann, J., Steier, P., Dittmar, T., Battin, T.J., 2012. Biogeochemically diverse organic matter in Alpine glaciers and its downstream fate. Nat. Geosci. 5, 710—714.

Sirivichi, G.M., Kaushal, S.S., Mayer, P.M., Welty, C., Belt, K.T., Newcomer, T.A., Newcomb, K.D., Grese, M.M., 2011. Longitudinal variability in streamwater chemistry and carbon and nitrogen fluxes in restored and degraded urban networks. J. Environ. Monit. 13, 288—303.

Stutter, M.I., Richards, S., Dawson, J.J.C., 2013. Biodegradability of natural dissolved organic matter collected form a UK moorland stream. Water Res. 47, 1169—1180.

Temnerud, J., Duker, A., Karlsson, S., Allard, B., Koehler, S., Bishop, K., 2009. Landscape scale patterns in the character of natural organic matter in a Swedish boreal stream network. Hydrol. Earth Syst. Sci. 13, 1567—1582.

Vannote, R.L., Minshall, G.W., Cummins, K.W., Sedell, J.R., Cushing, C.E., 1980. The river continuum concept. Can. J. Fish. Aquat. Sci. 37, 130—137.

Vannak, A., 2015. Linking River Sediment Physical Properties to Biofilm Biomass and

Activity. Ph.D. thesis. Universitat de Girona, Spain, p. 101.

Vazquez, E., Amalfitano, S., Fazi, S., Butturini, A., 2011. Dissolved organic matter composition in a fragmented Mediterranean fluvial system under severe drought conditions. Biogeochemistry 102, 59—72.

Vazquez, E., Ejarque, E., Ylla, I., Romaní, A.M., Butturini, A., 2015. Impact of drought-rewetting cycle on bioavailability of dissolved organic matter molecular weight fractions in a Mediterranean stream. Freshw. Sci. 34, 263—275.

Vidon, P., et al., 2010. Hot spots and hot moments in riparian zones: potential for improved water quality management. J. Am. Water Res. Assoc. 46, 178—298.

Waiser, M.J., Robarts, R.D., 2000. Changes in composition and reactivity of allochthonous DOM in a prairie saline lake. Limnol. Oceanogr. 45, 763—774.

Wollheim, W.M., Stewart, R.J., Aiken, G.R., Butler, K.D., Morse, N.B., Salisbury, J., 2015. Removal of terrestrial DOC in aquatic ecosystems of a temperate river network. Geophys. Res. Lett. 42, 6671—6679.

Wollheim, W.M., Vorosmarty, C.J., Peterson, B.J., Seitzinger, S.P., Hopkinson, C.S., 2006. Relationship between river size and nutrient removal. Geophys. Res. Lett. 33, L06410. http://dx.doi.org/10.1029/2006GL025845.

Zhou, Q.H., Cabaniss, S.E., Maurice, P.A., 2000. Considerations in the use of high-pressure size exclusion chromatography (HPSEC) for determining molecular weights of aquatic humic substances. Water Res. 34, 3505—3514.